Communication

Broad Spectral Domain Fluorescence Wavelength Modulation of Visible and Near-Infrared Emissive Polymersomes

P. Peter Ghoroghchian, Paul R. Frail, Kimihiro Susumu, Tae-Hong Park, Sophia P. Wu, H. Tetsuo Uyeda, Daniel A. Hammer, and Michael J. Therien

J. Am. Chem. Soc., **2005**, 127 (44), 15388-15390• DOI: 10.1021/ja055571b • Publication Date (Web): 18 October 2005

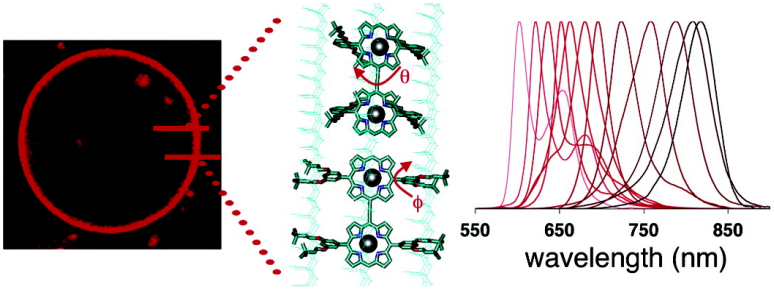

More About This Article

Additional resources and features associated with this article are available within the HTML version:

- Supporting Information
- Links to the 10 articles that cite this article, as of the time of this article download
- Access to high resolution figures
- Links to articles and content related to this article
- Copyright permission to reproduce figures and/or text from this article

View the Full Text HTML

J|A|C|S
COMMUNICATIONS

Published on Web 10/18/2005

Broad Spectral Domain Fluorescence Wavelength Modulation of Visible and Near-Infrared Emissive Polymersomes

P. Peter Ghoroghchian,[†,‡] Paul R. Frail,[‡] Kimihiro Susumu,[‡] Tae-Hong Park,[‡] Sophia P. Wu,[‡] H. Tetsuo Uyeda,[‡] Daniel A. Hammer,*[,†] and Michael J. Therien*[,‡]

School of Engineering and Applied Science, and Institute for Medicine and Engineering, University of Pennsylvania, 120 Hayden Hall, 3320 Smith Walk, Philadelphia, Pennsylvania 19104, and Department of Chemistry, University of Pennsylvania, 231 South 34th Street, Philadelphia, Pennsylvania 19104

Received August 15, 2005; E-mail: hammer@seas.upenn.edu; therien@sas.upenn.edu

Convergent advances in photonics and chemistry are enabling many promising optically based technologies for biomedical imaging and phototherapy.[1] Successful clinical application is dependent upon the continuing development of bright, nanometer-scale, long-wavelength visible and near-infrared (NIR) emissive organic materials.[1a,2] For deep-tissue fluorescence-based imaging, we have developed NIR-emissive polymersomes[3]—synthetic vesicles which stably incorporate numerous multiporphyrin-based NIR fluorophores[4] within their thick lamellar membranes. Polymersomes (50 nm to 50 μm diameter polymer vesicles) have been tailored to possess a rich diversity in material properties, including tunable in vivo circulation times, specific adhesiveness, environmental responsiveness, and biodegradability.[5] Here, we demonstrate that incorporation of an extended family of multi[(porphinato)zinc(II)] (PZn)-based supermolecular fluorophores gives rise to a rich photophysical diversity in emissive polymersomes, enabling emission energy modulation over a broad spectral domain. Moreover, controlling polymer-to-fluorophore noncovalent interactions finely tunes the bulk photophysical properties of these soft, supramolecular, optical materials.

A large body of literature focused upon the utilization of monomeric porphyrinoid compounds as photosensitizers has previously determined that noncovalent confinement in molecular assemblies greatly influences the sensitizer's photophysical properties.[6] Congruent with this work, we explored the absorptive and emissive signatures of polymersomes incorporating a variety of ethyne- and butadiyne-bridged (PZn)-based supermolecular fluorophores varying in macrocycle-to-macrocycle linkage topology. These bis- and tris(PZn) arrays (compounds **A**−**I**) that feature *meso*-to-*meso* (Figure 1), *meso*-to-β, and β-to-β conjugated linkages (Supporting Information, Figure S1) between the PZn units enable (i) extensive modulation of the magnitude of intermacrocycle excitonic and electronic interactions, (ii) substantial augmentation of emission dipole strength, and (iii) predictable control of fluorescence emission over a several thousand wavenumber energy domain that spans 600−1000 nm.[4]

Through cooperative self-assembly with amphiphilic diblock copolymers of poly(butadiene(1,2 addition)-*b*-ethylene oxide) (PEO_{30}−PBD_{46}), compounds **A**−**I** are stably incorporated, noncovalently, into vesicle membranes at high concentrations (5 mol % fluorophore:polymer). Note that these preparations of emissive polymersomes give rise to a heterogeneous distribution of vesicle diameters (ranging from 50 nm to 20 μm) that can be further processed (via sonication and membrane extrusion) into a homogeneous suspension post-assembly; 5 mol % of fluorophore loadings thus correspond to 650 and 10^8 copies of emitter, respectively, in the smallest (50 nm) and largest (20 μm) diameter polymersomes fabricated.[3] Confocal microscopy experiments support that, for each emissive polymersome formulation, compounds **A**−**I** are uniformly distributed exclusively within the hydrophobic bilayer membranes of these synthetic vesicles, displaying no evidence of macroscopic aggregate-domain formation or polymer/dye phase separation (Figure 1, Figure S1). Within these localized environments, long polymer chains constrain accessible chromophore conformations and control lateral and rotational diffusion. At 5 mol % loading, electronic spectral data indicate that the extent of interchromophoric interactions is limited; these well-dispersed membrane-embedded fluorophores experience nanometer scale separations, yielding uniformly fluorescent vesicles.

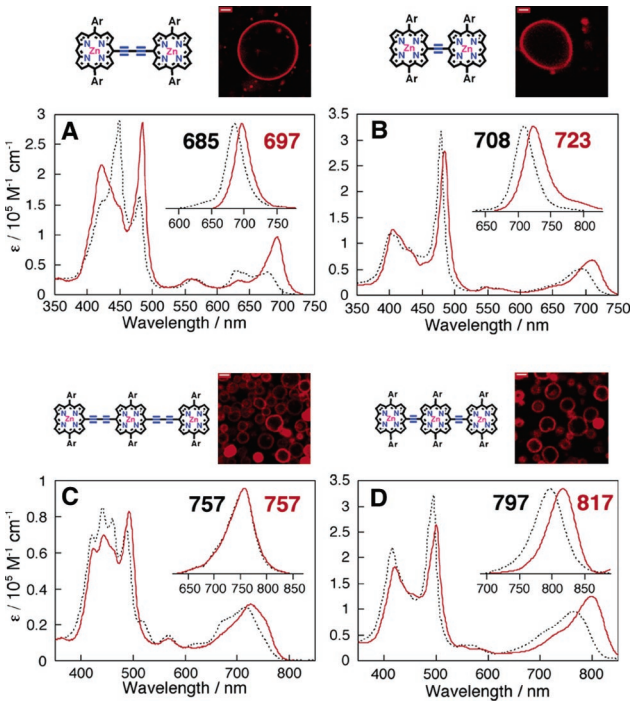

Figure 1. Ethynyl- and butadiynyl-bridged bis- and tris[(porphinato)zinc] arrays (**A**−**D**) that feature *meso*-to-*meso* linkage topologies between PZn units. Scanning fluorescence confocal microscope images of giant (5−20 μm) polymer vesicles feature compounds **A**−**D** loaded at 5 mol % concentrations within their lamellar membranes (scale bar = 10 μm). Electronic absorption and fluorescence emission (inset) spectra are for compounds **A**−**D** in THF (black) and of corresponding aqueous solutions of 100 nm diameter polymersomes that disperse these fluorophores (red).

Electronic absorption spectra of aqueous suspensions of small (100 nm diameter) emissive polymersomes (Figure 1, Figure S1, red) show that membrane-dispersed **A**−**I** possess absorptive signatures and light-harvesting characteristics remarkably similar

[†] School of Engineering and Applied Science.
[‡] Department of Chemistry.

10.1021/ja055571b CCC: $30.25

to those manifest for these species in dilute organic solvent (black). In general, relative to the optical properties observed in tetrahydrofuran (THF) solvent, vesicle-incorporated fluorophores **A**−**I** exhibit batho- and hyperchromic shifts of their lowest energy absorption manifolds, as well as red-shifted fluorescence bands (Supporting Information, Table S1). It has previously been established that, in bulk solvent, the extent of **A**−**I** spectral heterogeneity is a sensitive function of linkage topology, as steric effects largely dictate the allowable torsional angle range between macrocycle planes and the magnitude of PZn-to-PZn conjugative interactions.[4b,c,e] Within polymersome membranes, it is apparent that these rigid, conjugated, multichromophoric molecular architectures display reduced spectral heterogeneity relative to that displayed in organic solvent, consistent with a narrower PZn−PZn torsional angle distribution centered about a diminished mean macrocycle−macrocycle torsional angle.[4c,e] This membrane-driven chromophore organization effect is most pronounced in *meso*-to-*meso* linked fluorophores **A**−**D** (Figure 1).

The interactions of the chromophores' *meso*-aryl ring solubilizing substituents with polymer chains in the vesicles' bilayer membranes afford further modulation of their optical properties. As shown in Figure 2, the nature of intermembranous polymer-to-fluorophore interactions depends on the position and identity of the porphyrins' phenyl ring substituents. The diminished librational freedom of polymer chains within the bilayer controls packing and characteristic chromophore solvation. The polymersome membrane not only defines a dielectric environment for these fluorophores that differs from bulk organic solvent but also impacts the magnitude of the PZn-to-PZn interplanar torsional angle (θ) as well as the extent of conjugation between the macrocycle core and the 10- and 20-pendant aryl groups (ϕ) (Figure 2B). Figure 2C shows that varying aryl group substitution from a 3′,5′- to a 2′,6′-pattern converts overall chromophore geometry from a biconcave wedge to a cylinder; these substantive gross structural modifications, coupled with the selection of specific *meso*-phenyl ancillary substituents (Figure 2D), influence the local arrangement of polymer chains. Figure 2E shows the fluorescence bands of vis and NIR emissive polymersomes that incorporate emitters **A**−**I** (Figure 1, Figure S1) and variants differing in *meso*-aryl ring solubilizing substituents.

For a series of *meso*-to-*meso* butadiynyl- and ethynyl-bridged bis- and tris(PZn)-based supermolecular fluorophores, selection of specific *meso*-phenyl substitution patterns is used to tune their fluorescence band maxima in emissive polymersomes with added precision (Figure 3). In dilute THF solution, the position of the ancillary aryl 3,3-dimethyl-1-butyloxy substituent does not impact fluorophore optical properties; chromophores based on 10,20-diarylporphyrins having 2′,6′-disubstituted aryl rings exhibit the same absorptive and emissive signatures as those that feature 3′,5′-disubstituted *meso*-aryl groups (Figure 3, black). In polymersome environments, however, chromophores bearing 2′,6′-di(3,3-dimethyl-1-butyloxy)phenyl rings display fluorescence band hypsochromic shifts (Figure 3 blue), while the same chromophores possessing a 3′,5′-aryl substitution pattern exhibit bathochromically shifted emission bands relative to that observed in THF solvent (Figure 3, red). As tabulated in Figure 3A, these effects become more pronounced with the extent of coupling facilitated by the PZn-to-PZn linkage motif (ethynyl > butadiynyl); note that for *meso*-to-*meso* ethyne-bridged tris(PZn) fluorophore **4** this strategy regulates impressively the fluorescence signal over a 55 nm window centered at the benchmark emission band maximum observed in THF solvent (797 nm).

Modulating the amphiphilicity of these PZn-based fluorophores affords additional control over their optical properties within

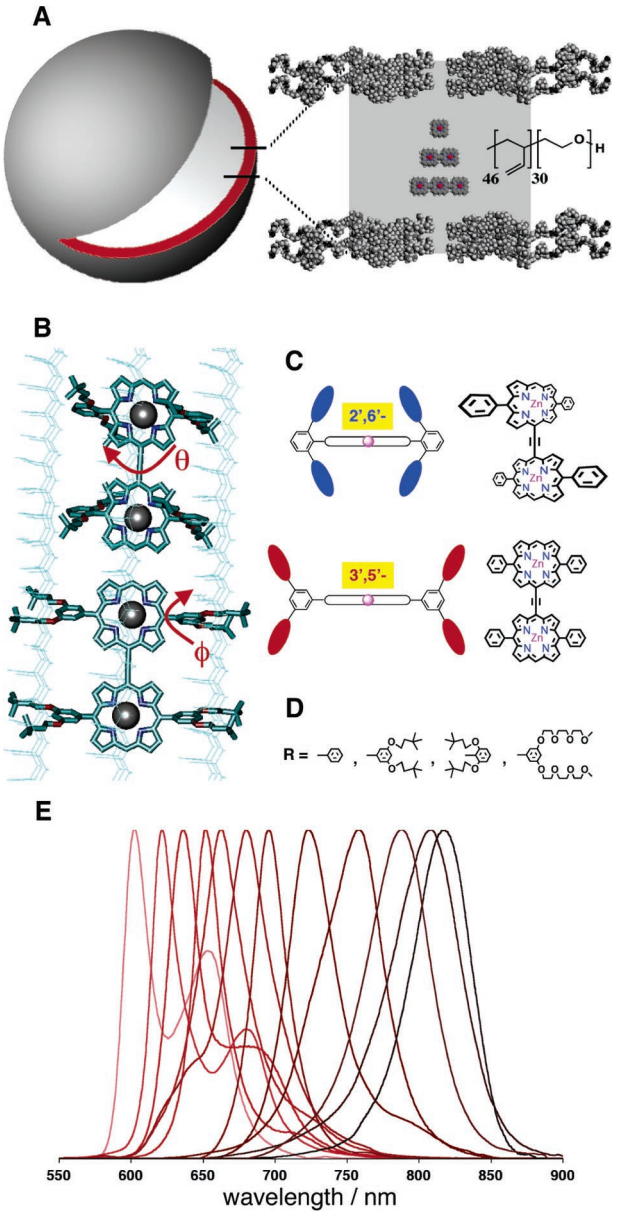

Figure 2. (A) Schematic of polymersomes incorporating mono-, bis-, and tris(PZn)-based chromophores. (B) Schematic representation of the interactions that modulate the degree of supermolecular conjugation, and the distribution and relative population of specific torsional angles for a given aryl-substituted multi(PZn)-based fluorophore; (θ) porphyrin-to-porphyrin interplanar torsional angle; (ϕ) torsional angle between the macrocycle core and the 10- and 20-pendant aryl groups. (C) Topological properties of 3′,5′- versus 2′,6′-substituted ethynyl-bridged bis(PZn) arrays. (D) Meso-phenyl ancillary substituents. (E) Fluorescence emission from visible and NIR-emissive polymersomes that incorporate fluorophores **A**−**I** (Figure 1, Figure S1) and variants differing in *meso*-aryl ring solubilizing substituents.

polymersome membranes. For example, replacement of *meso*-aryl ring 3′- and 5′-3,3-dimethyl-1-butyloxy substituents with 9-methoxy-1,4,7-trioxanonyl groups augments chromophore hydrophilicity; note, however, in THF solvent, the emission wavelength of *meso*-to-*meso* ethyne-bridged bis- and tris(PZn) chromophores is not impacted by this ancillary alkoxy group modification (Supporting Information, Figure S2). When dispersed in PEO_{30}−PBD_{46}-based polymersomes, the relative proportion of ancillary 3,3-dimethyl-1-butyloxy and 9-methoxy-1,4,7-trioxanonyl aryl substituents affects the emission energy, as well as the spectral breadth of the low-energy absorptive and emissive transitions of these supermolecular fluorophores (Figure S2). While it is difficult to segregate effects

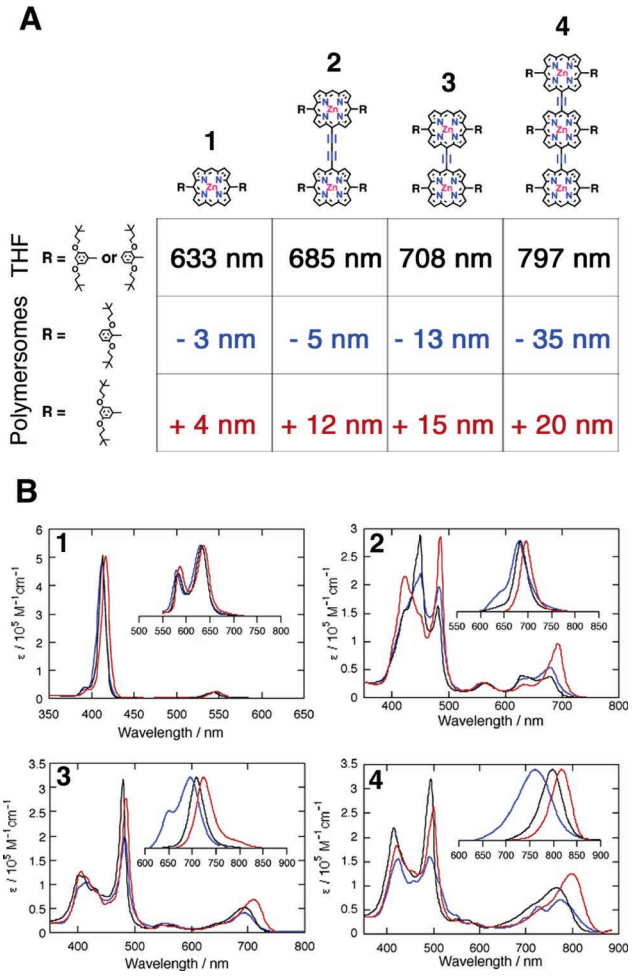

Figure 3. (A) Tabulated effects of 2′,6′- versus 3′,5′-substituted aryl groups on the absorption and emission of nanopolymersomes incorporating *meso*-to-*meso* butadiynyl- and ethynyl-bridged bis- and tris(PZn) arrays. (B) Corresponding absorption and fluorescence emission (inset) spectra.

due to polymer chain packing variations that derive from perturbations to the overall chromophore shape by replacement of 3,3-dimethyl-1-butyloxy groups with the larger 9-methoxy-1,4,7-trioxanonyl moiety, the modulations of emissive polymersome optical properties highlighted in Figure S2 likely originate from the nature of substituent-driven chromophore dispersion within the vesicle membrane. Hydrophobic 3,3-dimethyl-1-butyloxy groups are expected to preferentially disperse these PZn-based fluorophores into the hydrophobic core of the bilayer membrane (Figure S2), while increasing numbers of 9-methoxy-1,4,7-trioxanonyl groups should enhance the extent to which these chromophores are dispersed at the membrane environment defined by the interface of the hydrophilic PEO and hydrophobic PBD block fractions (Figure S2). Similar substituent-driven fluorophore dispersion effects are well established for other membrane probes.[6] Note that emissive polymersomes based on 9-methoxy-1,4,7-trioxanonyl-bearing chromophores display low energy absorptive and emissive bands with augmented spectral breadths relative to analogous vesicles that disperse identical fluorophores having exclusively 3,3-dimethyl-1-butyloxy ancillary substituents, consistent with the enhanced dielectric anisotropy of a membrane environment at the interface of hydrophilic and hydrophobic polymer block fractions.

Notably, within emissive polymersomes, spectral domain emission energy modulation is independent of fluorophore concentration; selection of fluorophore ancillary substituents predictably controls intermembranous physicochemical interactions and offers a facile tool for photophysical tuning that differs from well-established mechanisms for guest dissolution and π-stacking in polymeric host materials.[7] As many of these porphyrin-based fluorophores exhibit narrow emission bands (e.g., **A**−**D**: fwhm 700−1000 cm^{-1}) within the polymersome matrix, there exists an opportunity for their multiplexing within polymer vesicles and for their utilization in multifluorophore in vitro and in vivo imaging studies over the 650−900 nm spectral domain.[8] Finally, given ready isolation of homogeneous solutions of PEO_{30}−PBD_{46} vesicles having fixed diameters as small as 50 nm,[3] this work underscores that brightly fluorescent polymersomes define a unique nanoscale-emissive platform comprised entirely of soft matter.

Acknowledgment. This work was supported by a grant from the National Cancer Institute (NO1-CO-29008). M.J.T. and D.A.H. thank the MRSEC Program of the National Science Foundation (DMR-00-79909) for infrastructural support. D.A.H. also thanks the National Institutes of Health (EB003457-01), and P.P.G. acknowledges fellowship support from the NIH Medical Scientist Training Program and the Whitaker Foundation. The authors are grateful to Dr. One-Sun Lee for his assistance.

Supporting Information Available: Materials, experimental details, electronic absorption and emission spectral data. This material is available free of charge via the Internet at http://pubs.acs.org.

References

(1) (a) Weissleder, R.; Ntziachristos, V. *Nat. Med.* **2003**, *9*, 123−128. (b) Rudin, M.; Weissleder, R. *Nat. Rev. Drug Discovery* **2003**, *2*, 123−131.

(2) Sevick-Muraca, E. M.; Houston, J. P.; Gurfinkel, M. *Curr. Opin. Chem. Biol.* **2002**, *6*, 642−650.

(3) Ghoroghchian, P. P.; Frail, P. R.; Susumu, K.; Blessington, D.; Brannan, A. K.; Bates, F. S.; Hammer, D. A.; Therien, M. J. *Proc. Natl. Acad. Sci. U.S.A.* **2005**, *102*, 2922−2927.

(4) (a) Lin, V. S.-Y.; DiMagno, S. G.; Therien, M. J. *Science* **1994**, *264*, 1105−1111. (b) Lin, V. S.-Y.; Therien, M. J. *Chem.—Eur. J.* **1995**, *1*, 645−651. (c) Kumble, R.; Palese, S.; Lin, V. S. Y.; Therien, M. J.; Hochstrasser, R. M. *J. Am. Chem. Soc.* **1998**, *120*, 11489−11498. (d) Susumu, K.; Therien, M. J. *J. Am. Chem. Soc.* **2002**, *124*, 8550−8552. (e) Rubtsov, I. V.; Susumu, K.; Rubtsov, G. I.; Therien, M. J. *J. Am. Chem. Soc.* **2003**, *125*, 2687−2696.

(5) (a) Discher, B. M.; Won, Y. Y.; Ege, D. S.; Lee, J. C. M.; Bates, F. S.; Discher, D. E.; Hammer, D. A. *Science* **1999**, *284*, 1143−1146. (b) Discher, D. E.; Eisenberg, A. *Science* **2002**, *297*, 967−973. (c) Antonietti, M.; Forster, S. *Adv. Mater.* **2003**, *15*, 1323−1333. (d) Photos, P. J.; Bacakova, L.; Discher, B.; Bates, F. S.; Discher, D. E. *J. Controlled Release* **2003**, *90*, 323−334. (e) Lin, J. J.; Silas, J. A.; Bermudez, H.; Milam, V. T.; Bates, F. S.; Hammer, D. A. *Langmuir* **2004**, *20*, 5493−5500. (f) Bellomo, E. G.; Wyrsta, M. D.; Pakstis, L.; Pochan, D. J.; Deming, T. J. *Nat. Mater.* **2004**, *3*, 244−248. (g) Napoli, A.; Valentini, M.; Tirelli, N.; Muller, M.; Hubbell, J. A. *Nat. Mater.* **2004**, *3*, 183−189. (h) Meng, F. H.; Hiemstra, C.; Engbers, G. H. M.; Feijen, J. *Macromolecules* **2003**, *36*, 3004−3006. (i) Najafi, F.; Sarbolouki, M. N. *Biomaterials* **2003**, *24*, 1175−1182.

(6) Lang, K., Mosinger, J.; Wagnerova, D. M. *Coord. Chem. Rev.* **2004**, *248*, 321−350.

(7) Gilbert, A.; Baggott, J. E. *Essentials of Molecular Photochemistry*; Blackwell Science: Oxford, U.K., 1991.

(8) (a) Han, M. Y.; Gao, X. H.; Su, J. Z.; Nie, S. *Nat. Biotechnol.* **2001**, *19*, 631−635. (b) Wu, X. Y.; Liu, H. J.; Liu, J. Q.; Haley, K. N.; Treadway, J. A.; Larson, J. P.; Ge, N. F.; Peale, F.; Bruchez, M. P. *Nat. Biotechnol.* **2003**, *21*, 41−46. (c) Mahmood, U.; Tung, C. H.; Tang, Y.; Weissleder, R. *Radiology* **2002**, *224*, 446−51. (d) Gao, X. H.; Cui, Y. Y.; Levenson, R. M.; Chung, L. W. K.; Nie, S. M. *Nat. Biotechnol.* **2004**, *22*, 969−976.

JA055571B